



HAL
open science

The specificity of P band PolInsar data over vegetation

Pascale Dubois-Fernandez, Sébastien Angelliaume, Jean-Claude Souyris,
Franck Garestier, Isabelle Champion

► **To cite this version:**

Pascale Dubois-Fernandez, Sébastien Angelliaume, Jean-Claude Souyris, Franck Garestier, Isabelle Champion. The specificity of P band PolInsar data over vegetation. 3. International Workshop on Science and Applications of SAR Polarimetry and Polarimetric Interferometry (POLinSAR 2007), Jan 2007, Frascati, Italy. 8 p. hal-02823519

HAL Id: hal-02823519

<https://hal.inrae.fr/hal-02823519v1>

Submitted on 30 Jul 2020

HAL is a multi-disciplinary open access archive for the deposit and dissemination of scientific research documents, whether they are published or not. The documents may come from teaching and research institutions in France or abroad, or from public or private research centers.

L'archive ouverte pluridisciplinaire **HAL**, est destinée au dépôt et à la diffusion de documents scientifiques de niveau recherche, publiés ou non, émanant des établissements d'enseignement et de recherche français ou étrangers, des laboratoires publics ou privés.

THE SPECIFICITY OF P BAND POLINSAR DATA OVER VEGETATION

Pascale Dubois-Fernandez⁽¹⁾, Sébastien Angelliaume⁽¹⁾, Jean-Claude Souyris⁽²⁾, Franck Garestier⁽³⁾, Isabelle Champion⁽⁴⁾

(1) ONERA, DEMR, Centre de Salon de Provence, BA701, 13661 Salon Air cedex, France ,
Email: pdubois@onera.fr

(2) CNES, DCT/SI/AR, 18 Avenue Edouard Belin, 31401 Toulouse cedex 9, France

(3) CESBIO, 18 Avenue Edouard Belin, 31401 Toulouse cedex 9, France

(4) INRA, Unité Ephyse, Centre de recherche de Bordeaux BP81, 33883 Villenave d'Ornon cedex, France

ABSTRACT/RESUME

A polarimetric and PolInSAR analysis has been conducted on the Nezer forest (Southern France) at L and P band on high resolution SAR data acquired with the ONERA RAMSES system in January 2004.

The dataset was investigated for its potential for retrieval of forest parameters from SAR data using three different techniques:

- Radiometric inversion from the cross-polarized term,
- PolInSAR inversion based on the random-volume over ground model
- An approach based on the anisotropy parameter.

This paper concentrates on polarimetric and PolInSAR inversion. The observed linear regression between anisotropy and vegetation height is inverted and provides a RMS error of the order of 2m. This technique displays no saturation at P band.

The PolInSAR data behaviour over the forest is consistent with the RVoG model. The standard inversion described in the literature is modified to account for the higher expected penetration at P band, by selecting a given extinction coefficient or a range of extinction coefficients. The inversion results are precise to within 1.2m. When the baseline is properly selected, the extinction coefficient is a weak parameter.

The concept of Compact Polarimetry (CP) as proposed by JC Souyris [9] is explored in the context of PolInSAR inversion and the accuracy of the Compact PolInSAR inversion is shown to be very similar to the one obtained with the full polarimetry. A preliminary assessment of the ionospheric effect on such an inversion shows low sensitivity of the inversion to Faraday effects when the one-way rotation is less than 15°. The mode where the transmit wave is circularly polarised is extremely promising..

1. INTRODUCTION

The Nezer forest is constituted by parcels of pine trees, which are characterised by different tree ages. It is an artificial forest managed by the French agronomic research center (INRA), providing an accurate and extensive ground truth.

In this paper, we present the data set, we then propose a polarimetric inversion technique based on the anisotropy parameter, the potential of P band PolInSAR data for vegetation characterisation is presented and finally the concept of compact polarimetry is explored for PolInSAR applications.

In an earlier paper [1], we have presented the calibration procedure and the radiometric analysis performed at L and P bands.

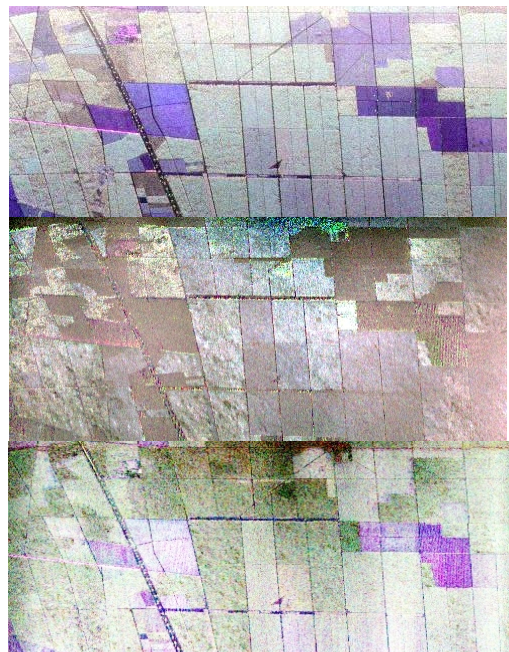


Figure 1: P-Band PolInSAR data set with the Sigma0 image (top), the interferometric phase (middle), the interferometric coherence (bottom) coded with HH in red, HV in green and VV in blue

2. THE DATASET

This site is a well monitored forest with uniform rectangular plots of pine trees.[2]. A large variety of tree heights and age can be found. The forest is maintained and has little undergrowth. The topography is almost flat.

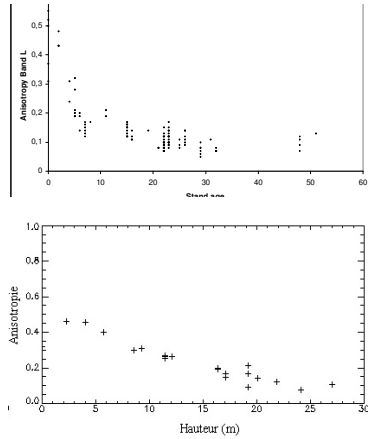


Figure 2: Anisotropy versus stand age at L band (top) and versus height at P band (bottom).

In **Figure 1**, the amplitude image and the interferometric complex coherence (argument and amplitude) for a P band couple are shown. In the phase image, the forest plots appear significantly higher than the bare surfaces.

3. POLARIMETRIC INVERSION

The different polarimetric parameters as proposed by Cloude and Pottier [3] are analysed and their potential for biomass inversion is assessed. One particular parameter appeared extremely promising: the anisotropy. Note that the L-band data presents a saturation level, whereas the P band analysis shows no such behaviour with a steady decrease in anisotropy as the age or height increases.

The full inversion was performed based on the relationship obtained by fitting a straight line through the points from **Figure 2** at P band [5]. The inversion results are presented in **Figure 3**, with a RMS error in height of the order of 2m.

The anisotropy parameter is an extremely interesting lead and needs to be fully evaluated on a large range of biomes to access its true characterization potential. The studies to be conducted will have to explore the effect of slope, the effect of species and the behaviour of such an indicator for denser forest. Furthermore, the anisotropy is a parameter which is extremely sensitive to thermal noise level as it is formed by using the second and the third eigenvalues obtained with the Cloude decomposition. The usual measure of SNR (signal to noise ratio) relies on the backscatter level in one channel. An analy-

sis on the forest data indicates that the third eigenvalue is often as much as 8dB below the first one. In order to provide a meaningful measure of the anisotropy, i.e., of the third eigenvalue, we conclude that the $NE\sigma_0$ over the co-pol channel must be at least 3dB below the level of the third eigenvalue, implying a SNR of at least 12dB in the co-polar channels.

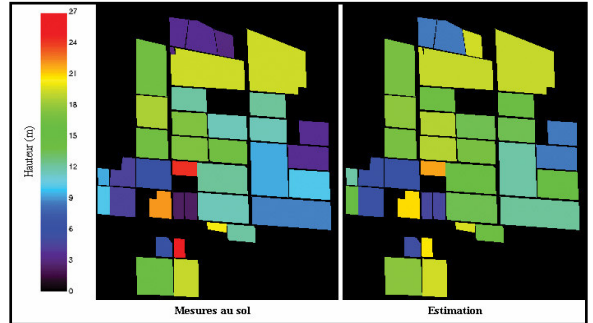


Figure 3: Ground measurements compared with Inverted forest height map from the anisotropy relation at P band

4. POLINSAR DATASET

Before any advanced analysis, it is essential to validate the PolInSAR calibration. This is done by analysing a bare surface.

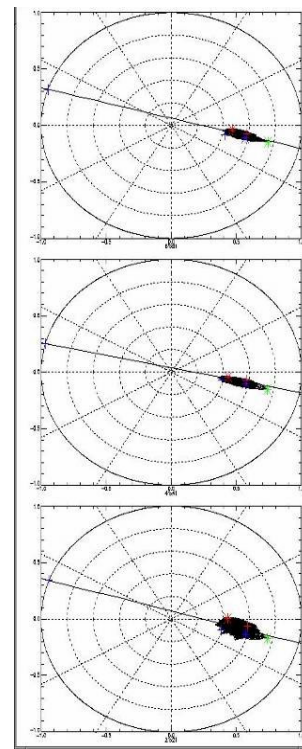


Figure 4: Coherency region corresponding to a bare surface for three window size 61x61; 41x41 and 21x21

As seen in **Figure 4**, the shape of the coherency regions are radial indicating consistent height information be-

tween the different polarisations. As expected, the standard deviation of the phase varies with the coherence and the number of independent samples in the window following the formula:

$$\sigma_{\phi}^2 = \frac{1}{2N} \frac{1-|\gamma|^2}{|\gamma|^2} \quad (1)$$

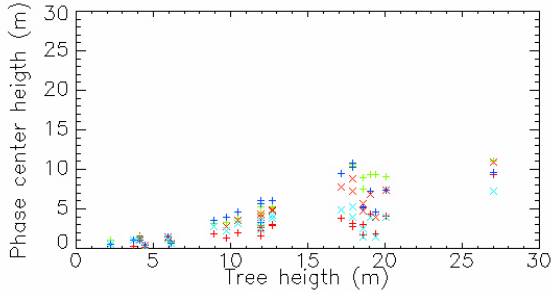


Figure 5: Polarimetric phase centers heights for different pine parcel heights. Color coding: HH, HV, VV, HH+VV, HH-VV

Fig. 5. displays the different polarimetric phase center heights as a function of the forest height. The forest height is obtained from age with an allometric relation adapted to the Nezer forest only [2]. We primarily observe that for forests higher than 6m, the polarimetric phase centers start to be widely dispersed.

Fig. 5. shows also that the relative positions of the polarimetric phase centers depend on the forest height and that the vertical position variations in function of the forest height appears to be continuous. This continuous vertical migration of the polarimetric phase centers during the forest growing has two origins. The first one is the height and size increase of the scattering objects (trunks, branches...) inducing a global elevation of the phase centres. This behaviour is observed for all the polarisation on **Fig. 5.** for the parcels lower than 15m. The second one is the creation or removal of coherent sources due to the size and geometry changes of these scattering objects. For example, it appears clearly on **Fig. 5** that the double bounce phase centre (associated with HH-VV polarisation) becomes the lowest one for highest forests. Indeed, the DBH (diameter at breast height) increases when the forest becomes older. It induces an augmentation of the dihedral formed by the intersection of trunk and soil surface. Consequently, a double bounce scattering source appears at this level or becomes stronger, leading to a variation of the corresponding phase center height.

5. RVOG MODEL AND P BAND

In the Random Volume Over Ground model [4] the signal backscattered from the forest is modelled as the combination of a ground contribution and a volume only contribution. The ground contribution can be the

surface scattering or double bounce effect linked to the tree trunks. The associated interferometric coherence is assumed to be one (no decorrelation). The interferometric coherence associated with the volume contribution is shown to be polarization independent (under the hypothesis that the attenuation is polarization independent) even though the corresponding backscattering depends on polarization [7]. When both contributions are present (they are assumed independent), the corresponding interferometric coherence γ_T can be written as:

$$\gamma_T = f(\gamma_g, \gamma_v) = \frac{P_g}{P_g + P_v} \gamma_g + \frac{P_v}{P_g + P_v} \gamma_v \quad (2)$$

where γ_v is the volume only coherence, γ_g is the ground coherence and P_g, P_v are the power of the ground scattering (including the attenuation through the canopy) and the power return from the volume. The powers are depending on polarisation and the total coherence is simply the weighed average of the two coherences. The locus of the interferometric coherence when polarisation varies, is along a line segment (see **figure 6**) between the point B (ground) and A (volume only). The inversion scheme as described by Cloude is as followed. (1) identify the line AB (2) Choose between the two intersection points with the unitary circle the one associated with the ground $e^{i\phi_0}$ (3) Select the furthest point from the ground as $e^{i\phi_0} \gamma_v$ (4) from γ_v , invert the vegetation height and attenuation.

$$\gamma_v = \frac{\int_0^{h_v} e^{uz} dz}{\int_{h_v} e^{vz} dz} = \frac{v}{u} \frac{[e^{uz}]_0^{h_v}}{[e^{vz}]_0^{h_v}} \quad \text{with } u = 2 \frac{\sigma_x}{\cos \theta} + ik_z \quad \text{and} \quad v = 2 \frac{\sigma_x}{\cos \theta} \quad (3)$$

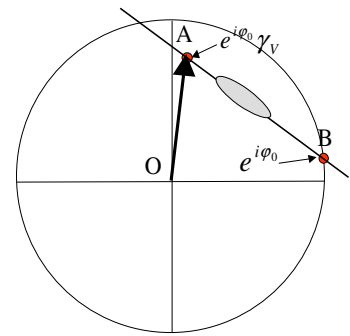


Figure 6: RvoG behavior. The grey ellipse is the one corresponding to the position of the interferometric coherence as the polarization varies

The parameter inversion is usually performed via a look-up table (LUT). In order for this scheme to be successful, one must be certain that **the volume only coherence** is observed for one polarisation. This can be true at X or C band but becomes more questionable as the frequency decreases. At P band, this is certainly rarely the case. On the complex unitary circle, the pseudo-ellipse will shift

towards the ground point as penetration increases. **Figure 7** is an illustration of what can happen at P Band when the ellipse doesn't contain point A associated with the volume only contribution.

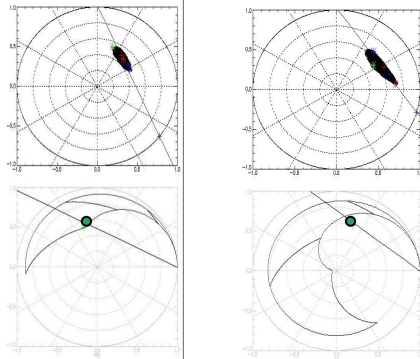


Figure 7: The complex unitary circle for two forest plots (age 48 on the left, age 11 on the right). The LUT is represented in the bottom figures and the green dot is the highest observed point.

For the young forest (right plots) and if we assume that the RvoG model is valid, we can conclude that the volume only contribution is not observed as the extreme (or highest) phase centre (green dot) in **Figure 7** is not inside the LUT (look-up table) area. In the following paragraphs, we describe how the initial procedure was modified for lower frequency acquisition.

6. ADAPTED INVERSION SCHEME

6.1 Straightforward approach

If the model is applicable, we know that the volume only coherence must lie on the fitted line to the left of the last observed coherence. We then assume a given attenuation coefficient; for P band we chose 0.3 dB/m from the analysis of a trihedral under canopy. The volume only contribution is determined as the intersection of the fitted line and the curve corresponding to the theoretical volume coherence associated with this attenuation coefficient (Eq 3). This position is then inverted for height.

In **Figure 8**, we present the corresponding inversion results. The lower vegetation plots are not inverted properly, certainly because little interaction occurs between the EM waves and the canopy at P band.

The inverted height is extremely stable within a forest plot as can be seen in **Figure 9** with an observed variation of the order of 1m.

6.2 Sensitivity analysis

The same approach was also followed for other attenuation coefficients ranging from 0.1 to 0.5 dB/m. The sensitivity of the inversion to the attenuation coefficient was found to be weak in our data set, certainly because for the studied baseline.

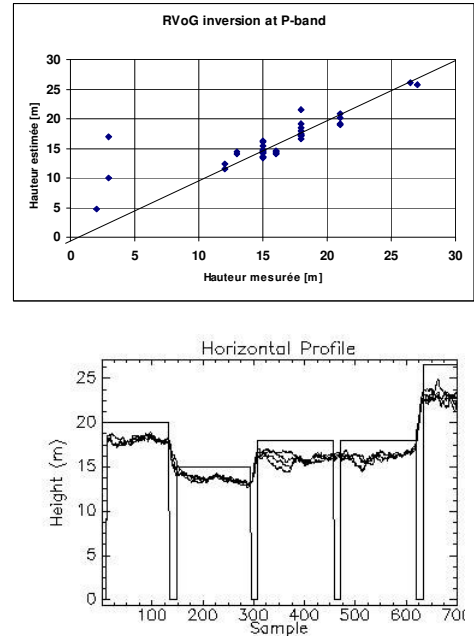


Figure 8: Inverted forest height versus ground measurements. RMS error of 1.2m (top figure), height profile (bottom figure)

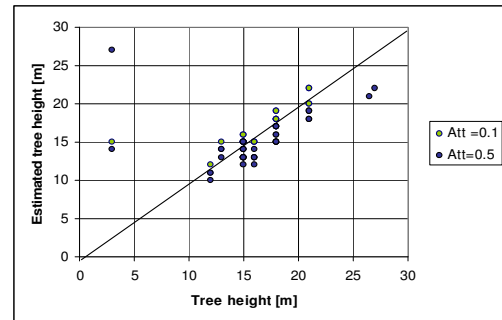


Figure 9: effect of the attenuation coefficient

In **Figure 9**, the inversion results for the two attenuation coefficients (0.1 and 0.5 dB/m) are provided. This low sensitivity can be explained by observing that for the study dataset, the baseline was such that in most cases the fitted line and the iso-height curve (obtained by varying the attenuation) associated with the volume only coherence are almost parallel.

7. COMPACT POLINSAR

The usual polarimetric SAR design architecture are built around the standard linear basis, H and V. On transmission, the radar interleaves pulses with a horizontal (H) and vertical (V) polarisation. On receive, both polarisations are received simultaneously. Full polarimetry has proved its increased potential compared to single channel acquisition. Several space-borne SAR systems in the near future will have this capability but will operate in the polarimetric mode only punctually. This is linked to the added complexity and timing constraints in the transmit chain when two orthogonal polarisation have to be transmitted on interleaved pulses. To maintain performance, the imaged swath is usually halved, resulting in a reduced coverage. One way around that is to restrict to dual-polarised mode as done by ENVISAT or ALOS-PALSAR. These satellites can transmit only one polarisation (H or V) and receive both H and V. This solution has proven very useful but can be improved. JC Souyris in [9-10] proposed an elegant alternative to the dual pol mode where instead of transmitting one of the two linear orthogonal polarised waves, the system transmits only one polarisation either H+V or circular (right or left circular, RC, LC). He called this mode compact polarimetry (CP).

He showed that the polarimetric information is well preserved for natural targets for which some symmetrical properties can be assumed. For these targets, he reconstructed an equivalent to the coherence matrix very similar to the one issued from full polarimetric data (FP). K Raney [11-12] followed a parallel axe of research and showed how the Compact Polarimetry Stokes parameters can provide information almost equivalent to the full polarimetry case. Other papers have also explored the same concepts [13-14]

7.1 Compact PolInSAR

We decided to test the potential of compact polarimetry on the PolInSAR inversion at P band.

Several modes were tested:

Name	Transmit	Receive
Dual-Pol 1	H	H,V
Dual-Pol 2	V	H,V
PC1(Pi/4 linear)	45°	H,V
PC2 (Pi/4 RC)	LC	H, V
PC3 (Circular)	LC	LC, RC

The measurements on the two receiving channels are then noted in a vector form, as follows:

$$\text{Dual-Pol 1: } \vec{k}_{D1} = (HH, HV)^T \quad (4)$$

$$\text{Dual-Pol 2: } \vec{k}_{D2} = (VV, VH)^T$$

$$\text{PC1: } \vec{k}_{P1} = (HH + HV, VV + HV)^T$$

$$\text{PC2: } \vec{k}_{P2} = (HH + jHV, jVV + HV)^T$$

$$\text{PC3: } \vec{k}_{P3} = (HH + 2jHV - VV, HH + VV)^T$$

In the three last cases, one constant factor ($1/\sqrt{2}$ or 2) is ignored in the rest of the paper. Note first that the last two cases (PC2 and PC3) can be considered as equivalent as

$$\vec{k}_{P3} = \begin{pmatrix} 1 & j \\ 1 & -j \end{pmatrix} \vec{k}_{P2} \quad (5)$$

In the first part of this paper, we have shown that the volume only coherence was in general not observed in the Landes forest at P band. The inversion then consists in fitting a line through the coherences and computing the intersection of this line with the volume only coherence associated with a given attenuation. This point provides the vegetation height.

The key step is therefore to produce this line. In the standard inversion with full polarimetric data, the loci of all interferometric coherences associated with the different polarisation states of the receiving and transmitting antennas is used to obtain the line. This is a 4 parameter space as the polarisation of each antenna can be parametrised with 2 parameters, the ellipticity and the orientation. In this compact polarimetry mode, the transmit polarisation is fixed resulting in a two parameter space corresponding to the polarisation state of the receiving antenna. Notice that because the reception occurs on two orthogonal polarisation, any receiving antenna polarisation can be synthesized from the data. In the compact PolInSAR inversion, we compute the loci associated with all the polarisation state of the receiving antenna (two parameter space) described as follows:

$$\gamma(\psi, \eta) = \frac{\langle k^{ref}(\psi, \eta) k^{int}(\psi, \eta)^* \rangle}{\sqrt{\langle k^{ref}(\psi, \eta) k^{ref}(\psi, \eta)^* \rangle \langle k^{int}(\psi, \eta) k^{int}(\psi, \eta)^* \rangle}}$$

$$\text{where } k(\psi, \eta) = \begin{pmatrix} \cos \psi \\ e^{j\eta} \sin \psi \end{pmatrix} \vec{k} \text{ and } \psi \in [0, 180]$$

$$\text{and } \eta \in [0, 180]. \quad (6)$$

This two parameter space is a sub-space of the full polarimetric four parameter space. The angular sector described by this sub-space in the unitary circle is included (therefore smaller) in the 4 parameter-space described by the full polarimetric loci of interferometric coherences. The inversion procedure described in the previous sections can then be applied to the sub-space of interferometric coherence corresponding to the compact polarimetric mode.

The compact PolInSAR inversion was evaluated as followed:

- The explored angular sector on the unitary circle is compared to the angular sector associated with the full polarimetric information
- The inversion is performed based on the cloud of points associated with $\gamma(\psi, \eta)$.

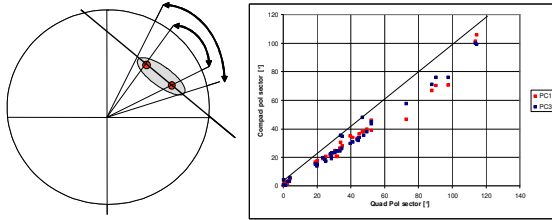


Figure 10: Angular extension of the interferometric coherences associated with PC1 et PC2 compared to the full polar case.

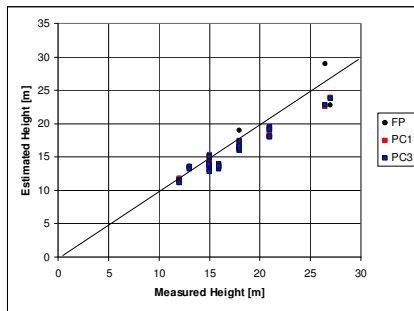


Figure 11: Compact PolInSAR inversion results PC1 et PC 2 compared to the full polar case

On our dataset and in the case of perfectly calibrated data, Compact PolInSAR performs as well as full polarimetric interferometry. Similar conclusions were found in the DP1 case. The DP2 case is not a good candidate. This results from the fact the VV and HV interferometric phase centers are very close to each other, providing a very small observable angular sector.

The results obtained on compact polarimetry are very encouraging but need to be taken one step further. At P band, propagation through the ionosphere introduces atmospheric effects (Faraday rotation, scintillation...) and up-to-now, most of the papers dealing with Faraday rotation correction stress the fact that correction cannot be performed on dual-pol data.

7.2 Effect of ionosphere

To initiate the problem, let's start by considering only the Faraday rotation effect. In the full polarimetry case, it has been modelled as [15-16]:

$$M = \begin{pmatrix} \cos \Omega & \sin \Omega \\ -\sin \Omega & \cos \Omega \end{pmatrix} \begin{pmatrix} HH & HV \\ HV & VV \end{pmatrix} \begin{pmatrix} \cos \Omega & \sin \Omega \\ -\sin \Omega & \cos \Omega \end{pmatrix}$$

where Ω is the one-way Faraday rotation.

As an example, we have written below the expression for the measurement vector k associated with the compact polarimetry mode PC1 in the presence of Faraday rotation.

$$\begin{bmatrix} HH(\cos^2 \Omega + j \sin \Omega \cos \Omega) + jHV + VV(-\sin^2 \Omega + j \sin \Omega \cos \Omega) \\ -HH(j \sin^2 \Omega + \sin \Omega \cos \Omega) + HV + VV(j \cos^2 \Omega - \sin \Omega \cos \Omega) \end{bmatrix}$$

Assuming the same ionosphere on the two acquisitions to be used in the interferometric processing, we first compute the measurement vectors associated with a given mode disturbed by the ionosphere and perform the inversion on these vectors.

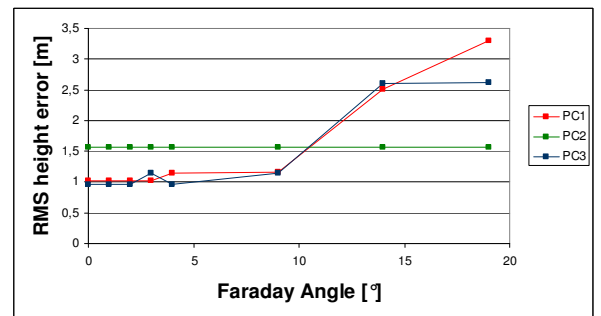


Figure 12: Influence of the one-way Faraday angle on the inversion from compact polarimetry with similar ionosphere on both measurements

For the PC2 (circular case) the two interferometric coherences are independent of the ionosphere. This is why there is no effect in the inversion. The other cases indicate that up to a (uncorrected) Faraday rotation of the order of 15° , the inversion is still performing well.

We now test the case where the two acquisitions are done through a different ionosphere (on two different days). This is more realistic even though the two acquisitions will be made at exactly the same time, which will minimize the differences.

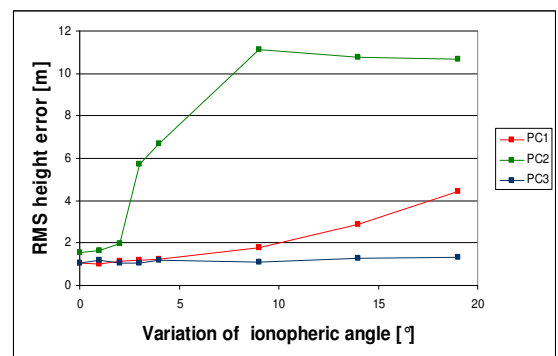


Figure 13: Influence of the one-way Faraday angle on the inversion from compact polarimetry with different ionosphere on both measurements

The same procedure is applied, with one measurement vector not disturbed while the other is perturbed by a given Faraday rotation.

In Fig 13, the inversion results are showing little sensitivity to the ionosphere for a Faraday rotation difference

of less than 15° . After 15° , the inversion results are degrading significantly. The green curve, corresponding to the circular case should be ignored. In our current implementation, we use only the two coherence vectors (the interferometric coherences corresponding to the two measurement channels) and we did not consider the 2 parameter space described in equation (6). This will be modified in the future work. In this preliminary implementation because the RR and RL coherences are very close to each other in the unitary circle, the inversion is very sensitive to any small variation.

7.3 Discussion

This preliminary analysis is extremely encouraging because it shows that over this dataset:

- The compact PolInSAR inversion works as well as the full polarimetric mode.
- The ionosphere has an effect but this effect can be neglected when the uncorrected Faraday rotation is less than 15° and when the differential Faraday rotation is less than 15° .

Further analysis are required

- To validate these results over a wider range of forest type and underlying topography,
- To develop specific ionospheric correction algorithm taking full advantage of the property of the compact polarimetry with a circular transmit wave.

When a circular wave is transmitted it propagates through the ionosphere while keeping its circular characteristic. The incident wave on the surface will be circular (assuming that the ionospheric effects are correctly described by the current model) whatever the ionosphere. The scattered field from the surface will therefore always correspond to the response of the surface to a circularly polarised wave. The propagation through the ionosphere will rotate the scattered field which will be received on two orthogonal antennas, meaning that for any Faraday rotation, the actual scattered field in response to a circular polarized wave is just a rotated version of the measured signal vector. This property is essential as it guaranties that the two parameter sub-space we talked about before is the same for any ionosphere, therefore will be the same for two acquisition acquired at different times. This does not hold when a linear polarised wave is transmitted. A straightforward example is the simple dual-pol case. A horizontally polarised wave is transmitted. Depending on the ionosphere, the surface can receive an H (no ionosphere) or V (a 90° Faraday rotation) polarised wave. The scattered fields will therefore be completely different and in that extreme case, PolInSAR analysis could not be performed.

One other main aspect which needs to be addressed is the calibration issue. How do we calibrate a CP system. K Raney pointed at some very interesting properties of

such a system and this needs to be followed through. [17]

8. CONCLUSION

We have presented a polarimetric inversion on P band data relying on the linear regression between the anisotropy parameter and the vegetation height.

We have found that Polinsar data can be successfully inverted using the Random Volume Over Ground (RvoG) model and an inversion procedure adapted to the P Band data, by assuming a known attenuation coefficient or a range of attenuation coefficients. The sensitivity to this parameter was observed to be weak given a proper baseline selection. The inversion proved to be performing very well at P band with a measured rms height error of 1.2m, therefore below the assumed ground measurement accuracy (Fig 8). The performance degrades significantly when the baseline is not adapted.

Compact PolInSAR was introduced and the first inversion results from compact PolInSAR were shown to be comparable to those associated with full polarimetry. The effect of the ionosphere was modelled and the preliminary assessment is very encouraging with a 15° range of ionosphere or differential ionosphere causing little to no degradation on the inversion. If this proved to be true for the majority of forest (including forest on sloping terrain), it could have an important impact on the design of a space-borne mission.

9. REFERENCES

- [1] P. Dubois-Fernandez., F Garestier, I. Champion, X Dupuis, P Paillou, " Ramses P band and L band campaign over the Nezer forest: calibration and polarimetric analysis", EUSAR2006 symposium, Dresden, Germany, May 2006
- [2] I. Champion, Loustau, D., Bert, D., Porté, A., Guédon, M., Jean-Courcier, F., Lagane, F., Lambrot, C., Lardit, A., Sartore, M., 2001, Tree architecture determination in remote sensing analytical models : The Bray experiment. Int. J. Remote Sensing, Vol. 22, N. 9, 1827-1843.
- [3] P. Dubois-Fernandez, X. Dupuis, F. Garestier, "PolInSAR calibration of deramp-on-receive system: example with the RAMSES airborne system," Canadian Journal of Remote sensing., Volume 31 Number 1, February 2005. .
- [4] S.R. Cloude, E. Pottier, " An Entropy Based Classification Scheme for Land Applications of Polarimetric SAR ", IEEE Transactions on Geoscience

and Remote Sensing, Vol. 35, No. 1, pp 68-78 ,
January 1997

- [5] F. Garestier, I. Champion, P. Dubois-Fernandez, P. Paillou and X. Dupuis “ Polar and PolInSAR analysis of pine forest at L and P band on high resolution data”; IGARSS’05, Seoul, South Korea
- [6] S.R. Cloude and K.P. Papathanassiou, “A three stage inversion process for polarimetric SAR interferometry”, IEE proceedings, Radar, sonar and Navigation, Vol. 150, Issue 03, June 2003, pp 125-134
- [7] R. Treuhaft, S. Madsen, M. Moghaddam, and J. van Zyl, “Vegetation characteristics and underlying topography from interferometric radar”, Radio Science, Vol 31, Number 6, pp 1449-1485, Nov-Dec 1996
- [8] F. Garestier, “Evaluation du potentiel de la technique PolInSAR pour l’estimation des paramètres physiques de la végétation en conditions spatiales”, PhD thesis manuscript, 2006
- [9] JC Souyris, P Imbo, R Fjortoft, S. Mingot and JS Lee, « Compact polarimetry based on symmetry properties of geophysical media : The $\pi/4$ mode », IEEE TGRS Vol 43, N°3, March 2005, DOI10.1109/TGRS.2004.842486
- [10] JC Souyris, N Stacy, T Ainsworth, JS Lee, P Dubois-Fernandez, “SAR Compact Polarimetry for Earth Observation and Planetology: Concepts and Challenges”, Proceedings of POLINSAR 2007, <http://earth.esa.int/workshops/polinsar2007>.
- [11] K Raney, "Hybrid polarimetric SAR Architecture", Proceedings IGARSS'06 , July 2006
- [12] K Raney, "Dual-Polarized SAR and Stokes Parameters," *IEEE Geoscience and Remote Sensing Letters*, vol. 3, pp. 317-319, 2006.
- [13] N. Stacy, M. Preiss, "Compact polarimetric analysis of X band SAR data", in. Proc. EUSAR'06, Dresden, Germany, May 2006
- [14] T Ainsworth et al., “Analysis of Compact polarimetry Imaging Modes’ Proc. of POLINSAR07, <http://earth.esa.int/workshops/polinsar2007>.
- [15] A. Freeman and S. Saatchi, “On the detection of Faraday Rotation in linearly polarized L-Band SAR backscatter signatures”, IEEE TGRS Vol 42 N°8, August 2004 DOI10.1109/TGRS.2004.830163
- [16] P. Wright, S. Quegan, N. Wheadon and C. David Hall, “Faraday rotation effects on L-Band spaceborne SAR data” , IEEE TGRS Vol 41 N°12 December 2003 DOI10.1109/TGRS.2003.815399
- [17] K Raney, “Decomposition of Hybrid-Polarity SAR data”, Proceedings of POLINSAR07, <http://earth.esa.int/workshops/polinsar2007>

10. Acknowledgements:

This work was made possible by the active support of ESA and CNES. We are thankful to Keith Raney for the constructive discussions around a barrel of beer in Frascati. Our gratitude goes to the RAMSES team who acquired and processed the data.